Pergamon

Journal of Structural Geology, Vol. 18, No. 6, pp. 803 to 818, 1996

0191-8141/96 $15.00 + 0.00

PII: S0191-8141(96)00001-6

Origin of the Hafit structure: implications for timing the Tertiary deformation in the Northern Oman Mountains

MOHAMMED WARRAK

Department of Geology, Kuwait University, P.O. Box 5969, Safat 13060, Kuwait

(*Received* 3 *May* 1995; *accepted in revised form* 8 *January* 1996)

Abstract—The Hafit structure belongs to a group of large-scale, post-obduction periclines that deform the Late Cretaceous–Tertiary sediments of the Oman Mountains Foredeep. Due to one-sided compression from the ENE, the Hafit structure grew as a detachment fold above a basal decollement which is probably located in the Upper Cretaceous Lower Fiqa shale. Its reversed vergence, back thrust and the folds superposed on its limbs, are explained as being caused by simple shear modification of the original structure. The interpretation that the Hafit structure and other foreland folds in the Northern Oman Mountains have resulted from a Zagros-related late Eocene–Miocene compressional event, is at variance with the stratigraphical and sedimentological evidence from the Hafit area. This evidence shows that the Hafit structure grew synchronously with sedimentation from just before the Middle Eocene, until the end of the Miocene, whilst the related structures to the east of it were initiated at the beginning of the Palaeocene. With further evidence of a similar early start to the Tertiary deformation emerging from other parts of the Northern Oman Mountains, it becomes necessary to push back the date of initiation of the Tertiary compressional event to the Palaeocene and to set it apart from the Plio-Pleistocene Zagros deformation.

INTRODUCTION

The Oman Mountains of SE Arabia were formed through the obduction of a slice of oceanic crust and upper mantle, together with ocean basin and slope sediments and volcanics, onto the eastern continental margin of the Arabian Platform during the Late Cretaceous (Glennie *et al.* 1974). As a consequence of the loading of the Arabian Platform, a foredeep developed along the western flank of the obducted allochthon and was filled with Late Cretaceous–Tertiary sediments (Boote *et al.* 1990, Warburton *et al.* 1990). These sediments were deformed in post-obduction time and formed a group of large-scale periclinal folds fringing the arcuate western edge of the Northern and Central Oman Mountains. The Hafit structure, situated at the divide between the Northern and Central Oman Mountains at a distance of about 20 km to the west of the edge of the allochthon, is one of the most spectacular of these folds (Fig. 1). Apart from its unusual size (29 km long, 4 km wide and 1160 m high), its vergence is in the opposite direction to the general WSW vergence and inferred transport direction of all the other folds in the region.

Although the Hafit structure has been studied by many oil-company geologists and industrial consultants since 1936, the only available account from such studies is that of Hunting (1979), who gave a brief structural description of the northern (U.A.E.) half of the mountain together with three interpretative cross-sections. In spite of the increased number of recent studies dealing with the geology of the Northern Oman Mountains (e.g. Searle *et al.* 1983, Searle 1985, 1988a,b, Dunne *et al.* 1990), no detailed description of the Hafit structure has been published. Warrak (1986), however, in his study of the structural evolution of the Al Ain region, outlined its main geometrical features, and later (Warrak 1987) presented evidence to indicate that it developed synchronously with sedimentation from just before the Middle Eocene (late Early Eocene) until the end of the Miocene. These conclusions are at odds with the idea held by many workers (Hunting 1979, Boote *et al.* 1990) that the Hafit structure formed solely as a result of post-Miocene movements.

This paper describes the geometrical features of the Hafit structure in detail, and then uses both the structural and stratigraphic evidence to construct a model that is consistent with the field observations, to explain its origin and special features (viz. its reversed vergence, early time of initiation and its development synchronously with sedimentation), and also to account for the origin of the neighbouring structures in the region. Detailed mapping (1:20,000, 1:10,000 and 1:5000) and collection of stratigraphic and structural data have been made of the Hafit structure. The results were used to compile a final geological map at a scale of 1:50,000 which is to be published later. A simplified version of this map is shown in Fig. 2 and the rock units of the Hafit structure, their ages and stratigraphic relationships are shown in Table 1.

GEOMETRY

The Hafit structure can be described as a composite anticlinal structure consisting of two en échelon anticlines with opposing plunges; the main anticline in the south forms the bare mount (Jebel) Hafit itself, hence the name 'Jebel Hafit anticline', and the other to the north, the 'Al Ain anticline', which is partially exposed within

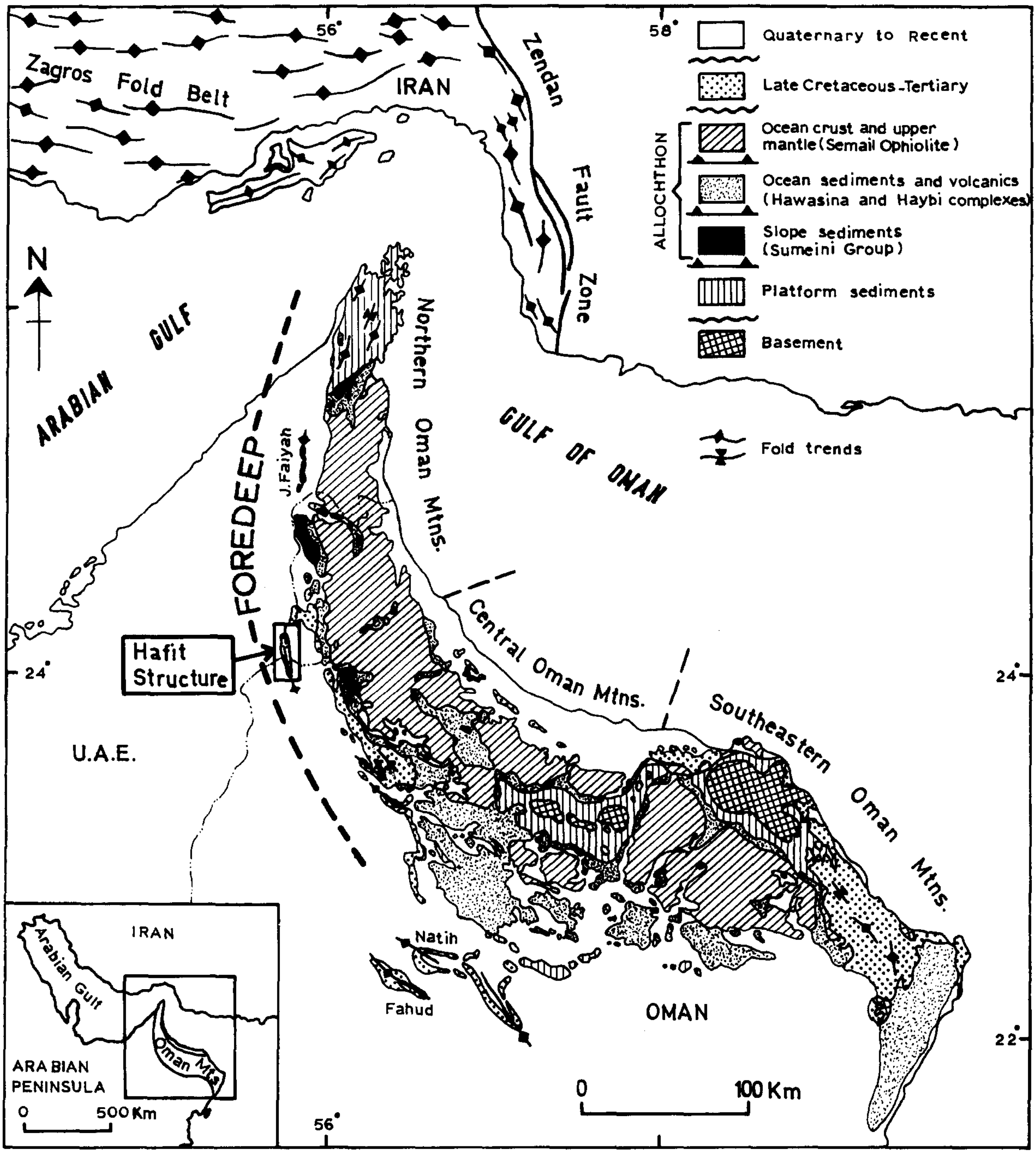

Fig. 1. Geological map of the Oman Mountains showing location of the Hafit structure. Based on Glennie *et al.* (1974), Coleman (1981) and Boote *et al.* (1990).

the southern outskirts of Al Ain city. These two anticlines are linked in a simple zigzag pattern by a doubly plunging syncline, 'Rwaidhat syncline' (Fig. 2). At higher levels in the folded succession (A_2 and above), however, the two anticlines coalesce to form one larger anticline with a deflection in the hinge line. This type of linkage has been described from the foothills of the Canadian Rockies by Dahlstrom (1970), who considered the simple zigzag pattern to be the basic form of one single model of en échelon linkage, which changes upwards to another form in which the en échelon separation is reflected by a small deflection of the anticlinal hinge line and a gentle saddle in the plunge.

Jebel Hafit anticline

The Jebel Hafit anticline is a long (24 km) and narrow (about 4 km exposed width) asymmetric, ENE-facing, 'whale-back' pericline, which rises to 860 m above the surrounding plains. It has a core of Early–Middle Eocene limestone (R-D_1^L), which is enveloped at its opposing ends by incomplete elliptical ridges made up of limestones belonging to the younger units (D_3,A_2) with marl filling the lower ground between (Fig. 2).

Detailed examination of the fold reveals that it consists of a body and two terminations that plunge in opposite directions (Fig. 3). The body is a broad-crested NNW–

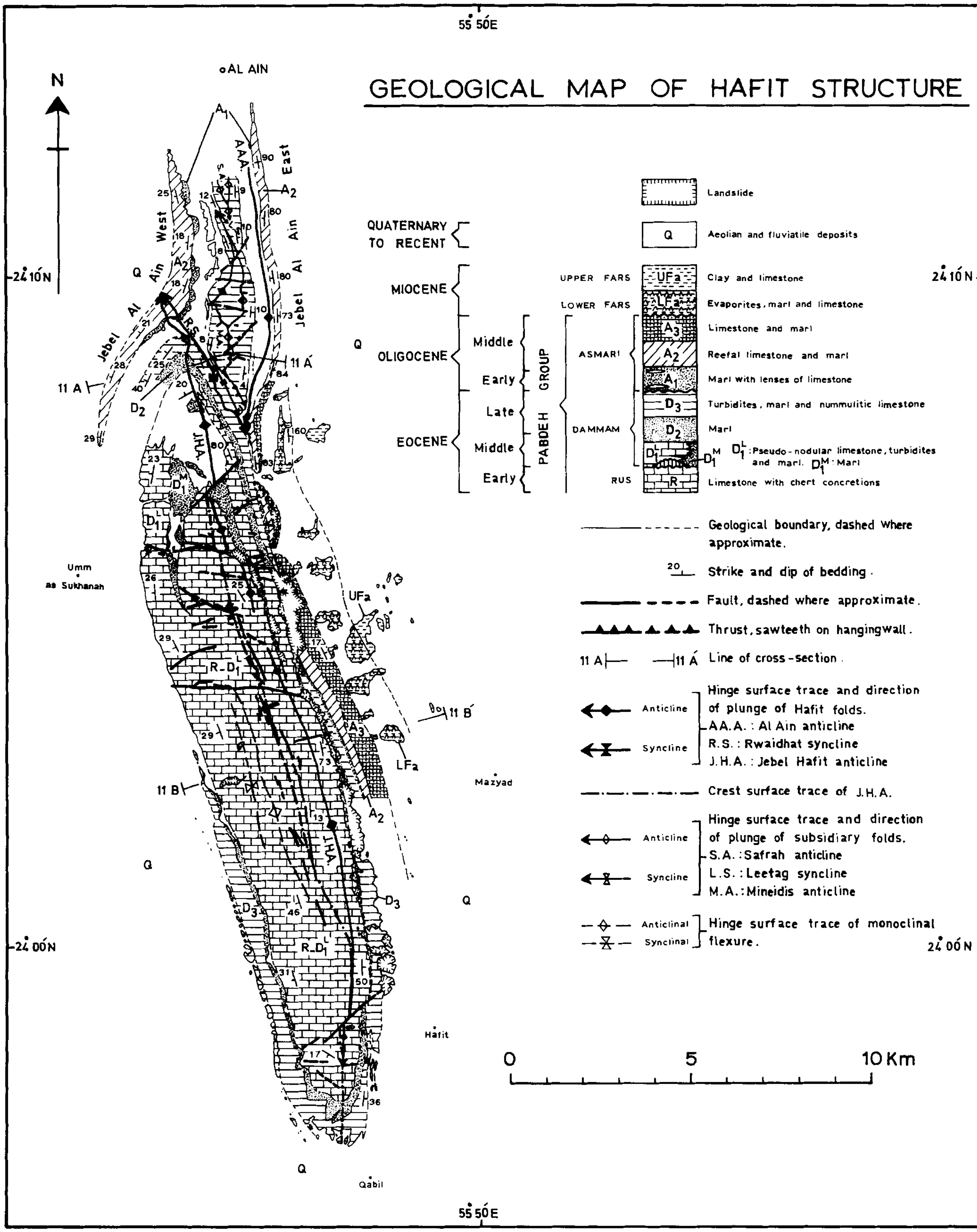

Fig. 2. Geological map of the Hafit structure.

SSE trending anticline having a steeply inclined or overturned eastern limb, and a gently WSW-dipping western limb. It is double-hinged in its middle part due to the presence of a narrow zone of monoclinal flexuring that affects the top of the western limb. Within this zone, which is nearly parallel to the main hinge line, the dip of the strata becomes steep and sometimes vertical, and then returns to its original attitude (Figs. 2 and 11, cross-section BB′). The strike of the bedding in the body maintains a near constant orientation and the hinge lines

Table 1. Surface and subsurface stratigraphic succession within the Hafit structure. Ages of the surface Tertiary rocks are based on Hunting (1979), Cherif & El Deeb (1984) and Hamdan & Bahr (1992). Ages and formations of the subsurface Tertiary and Cretaceous rocks are after Patton & O'Connor (1988) and Boote *et al.* (1990)

		AGE		FORMATION	UNIT SYMBOL	LITHOLOGY AND THICKNESS
SURFACE		QUAT. TO RECENT			Q	Aeolian sand, fluviatile and desert plain deposits.
SURFACE	TERTIARY	MIOCENE		Upper Fars	UFa	Gypsiferous clay and chalky limestone.(>250m)
SURFACE	TERTIARY	MIOCENE		Lower Fars	LFa	Celestite, gypsum, marl and marly limestone. (350-800m) ~~ Unconformity ~~
SURFACE	TERTIARY	MIDDLE OLIGOCENE	PABDEH GP.	Asmari	A_3	A_3: Fossiliferous marl, oolitic, bioclastic, and marly limestones and marl. (85-160m)
SURFACE	TERTIARY	OLIGOCENE	PABDEH GP.	Asmari	A_2	A_2: Algal boundstone, inter-reef detritus, bioclastic limestone and marl. (**Max. 210m**)
SURFACE	TERTIARY	EARLY OLIGOCENE	PABDEH GP.	Asmari	A_1	A_1: Gypsiferous marl with lenses of bioclastic limestone near the upper and lower contacts. (Av. 180m) ~~ Unconformity ~~
SURFACE	TERTIARY	LATE EOCENE	PABDEH GP.	Dammam	D_3	D_3: Jebel Hafit anticline. Turbidites, marl and nummulitic limestone along the western limb, changing to bioclastic limestone and marl along the eastern limb. Mineidis anticline. Nummulitic limestone and marl. (Av. 250m)
SURFACE	TERTIARY	LATE EOCENE	PABDEH GP.	Dammam	D_2	D_2: Marl; the upper part is criss-crossed with gypsum veins. (150m)
SURFACE	TERTIARY	MIDDLE EOCENE	PABDEH GP.	Dammam	D_1^L, D_1^M	D_1^L: Pseudo-nodular limestone and turbidites changing to predominantly marl and nummulitic banks in the north. Debris flows occur towards the top of the unit along the northerly end of the eastern limb of Jebel Hafit anticline. Western limb (200-400m). Eastern limb (125-380m). D_1^M: Marl with beds and lenses of marly limestone. (0-350m).
SURFACE	TERTIARY	EARLY EOCENE	PABDEH GP.	Rus	R	Pseudo-nodular limestone with chert concretions, marly limestone and marl. Dolomite and bioclastic limestone occur at the crest zone of Jebel Hafit anticline, whilst at the tip of its northern termination, the upper (30m) of the unit consists of debris flows and slumped sheets.
SUBSURFACE	TERTIARY	PALAEOC.	PABDEH GP.	Umm Er Radhuma	UR	Marly limestone and marl. ~~ Unconformity ~~
SUBSURFACE	CRETACEOUS	MAAST.	ARUMA GP.	Simsima	S	Shallow-water limestone.
SUBSURFACE	CRETACEOUS	CAMP.	ARUMA GP.	Upper Fiqa / Juweiza	UFi / J	Marl (Upper Fiqa facies) and coarse lithoclastics (Juweiza facies).
SUBSURFACE	CRETACEOUS	SAN. CON.	ARUMA GP.	Lower Fiqa	LFi	Shale ~~ Wasia_Aruma Break ~~
SUBSURFACE	CRETACEOUS	TUR. CEN.	WASIA GP.	Shilaif { Mishrif	SHi { MI	Platform carbonates.
SUBSURFACE	CRETACEOUS	ALB.	WASIA GP.	Mauddud	MA	
SUBSURFACE	CRETACEOUS	ALB.	WASIA GP.	Nahr Umr	NU	
SUBSURFACE	CRETACEOUS	APT. BAR.	THAM. GP.	Shuaiba	SHu	

Fig. 3. Map and equal-area projections of bedding poles for the Jebel Hafit anticline. The map shows the segments of the anticline, location of sub-areas which are shown numbered, hinge and crest surfaces traces and orientation of fold axes and crestal axes of terminal cones. 1. Equal-area projection of bedding poles for sub-area 1 excluding the part of the eastern limb which is affected by subsidiary folds. The poles lie in a field defined by small circles about a cone axis plunging 60°–317° with an apical angle varying from 42° (a cone with crestal plunge 41°–332°) to 94° (a cone with crestal plunge 16°–341°). 1′. Equal-area projection of bedding poles of the eastern limb in sub-area 1, showing the effect of the subsidiary folding. 3. Equal-area projection of bedding poles for sub-area 3. The poles lie in a field defined by small circles about a cone axis plunging 79°–349° with an apical angle varying from 108° (a cone with crestal plunge 25°–349°) to 135° (a cone with crestal plunge 11°–349°). 15. Equal-area projection of bedding poles for sub-area 15. The poles lie in a field defined by small circles about a cone axis plunging 44°–190° with an apical angle varying from 49° (a cone with crestal plunge 21°–180°) to 76° (a cone with crestal plunge 8°–176°).

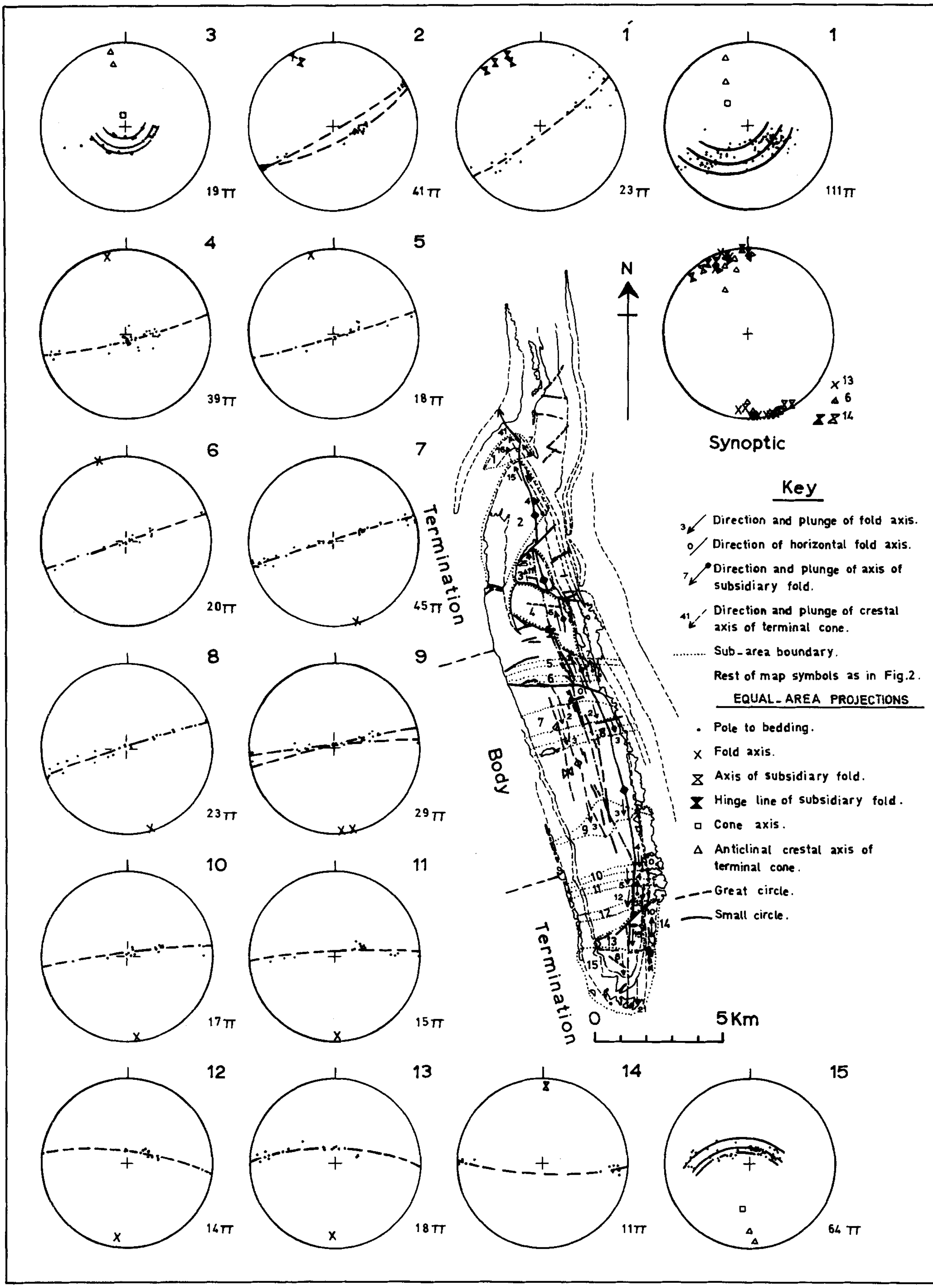
3
19π
2
41π
1'
23π
1
111π
4
39π
5
18π
6
20π
7
45π
8
23π
9
29π
10
17π
11
15π
12
14π
13
18π
14
11π
15
64 π
Synoptic
x 13
▲ 6
⧗ 14
N
Termination
Body
Termination
0
5 Km
Key
Direction and plunge of fold axis.
Direction of horizontal fold axis.
Direction and plunge of axis of subsidiary fold.
Direction and plunge of crestal axis of terminal cone.
Sub-area boundary.
Rest of map symbols as in Fig.2.
EQUAL-AREA PROJECTIONS
Pole to bedding.
Fold axis.
Axis of subsidiary fold.
Hinge line of subsidiary fold.
Cone axis.
Anticlinal crestal axis of terminal cone.
Great circle.
Small circle.

Fig. 3.

are nearly parallel with plunge values not exceeding 3° towards NNW or SSE, with a gentle culmination between (Fig. 3, sub-areas 5,6,7,8 and 9). Consequently, the body segment of the Jebel Hafit anticline is nearly cylindrical.

In the two terminations, however, the fold becomes increasingly non-cylindrical. One limb changes its trend, whilst the other continues with the trend of the body. As a result, the hinge lines gradually swing towards a N–S direction and progressively increase in plunge value (Fig. 3, sub-areas 4, 10, 11 and 12). At the tips of the terminations, the fold becomes completely non-cylindrical; the poles to bedding do not show a simple great circle distribution on equal-area projections, but scatter in broad zones with small circle affinities that indicate a complex conical geometry (Fig. 3, sub-areas 1, 3 and 15). In each of these sub-areas, the bedding poles lie in a field which is best fitted by a number of small circles about a common inclined cone axis, thus indicating that the fold surface can be described by a number of cones, whose apical angles increase continuously as the limb dips decrease towards the crest line. This is compatible with the opening out of the cones towards a near planar attitude due to the effect of a steeply plunging compressive strain. In sub-area 2 (Fig. 3), a similar pattern of small circle distribution of bedding poles could not be established due to the lack of measurements in the hinge zone area of the termination, but a best-fit great circle is drawn instead.

The above-described pattern of elliptical terminations with inclined circular cones is interpreted as having resulted because of non-uniform shortening by buckling and post-buckle flattening in accordance with the model proposed by Webb & Lawrence (1986), to explain a similar pattern of conical fold terminations in periclinal folds in the Bannisdale Slates of the English Lake District. Non-uniform shortening in the Jebel Hafit anticline is also indicated from estimates of finite shortening, which are determined by analysing the divergence of poles around the small circles in the equal-area plots of the terminations. This method (Nicol 1993), which assumes parallel folding and no significant layer-parallel shortening, gives the following shortening estimates; 19% in sub-area 3, 14.2% in sub-area 1 and 10.4% in sub-area 15.

The geometry of the Jebel Hafit anticline, as described earlier, is further complicated by two features. First, the presence of gentle to open folds superposed on the eastern limb of the anticline, and which cause the bedding on that limb to change dip from E to W after passing through the vertical. These folds—referred to here as subsidiary folds—have sub-horizontal to gently inclined hinge surfaces and sub-horizontal to gently plunging hinge lines. They are sometimes associated with sub-horizontal minor thrusts, and their hinge lines are nearly coaxial with the axes of the Jebel Hafit anticline (Fig. 3, synoptic diagram). The second feature is the displacement of the fold hinge line by conjugate strike-slip faults consisting of one WNW-trending sinistral set and a NE-trending dextral set.

Al Ain anticline

The general form of this anticline is that of an open, inclined fold with a steep to vertical eastern limb and a slightly curved, gently west-dipping to horizontal western limb. The hinge surface trace trends approximately N–S just to the west of Jebel Al Ain East (Fig. 4). The two limbs of the Al Ain anticline have subsidiary folds superposed on them. The subsidiary folds on the eastern limb, which can be seen in the Asmari limestone (A_2) of Jebel Al Ain East, are similar in form to the subsidiary folds superposed on the eastern limb of the Jebel Hafit anticline and, like them, cause the bedding to change its dip direction from east to west after passing through the vertical (Fig. 4). The subsidiary folds on the western limb are gentle and give the Al Ain anticline the appearance of a double-hinged fold. As can be seen in Figs. 2 and 4, there are two en échelon, N–S trending subsidiary anticlines, a large one to the south (Mineidis anticline), and a smaller one to the north (Safrah anticline). The Mineidis and Safrah anticlines are linked in a simple zigzag pattern by a doubly plunging, NW–SE trending subsidiary syncline (Leetag syncline).

Mineidis anticline

This is a doubly plunging conjugate anticline with rounded hinge zones, a 'box fold' as defined by Ramsay & Huber (1987). It consists of a N–S trending body and two asymmetrical terminations that plunge NW for the northern termination and mainly SE for the southern termination (Fig. 5). The box geometry of the body is clearly seen in its northern half (Fig. 5, section aa'); toward the south, however, erosion has removed the roof, thereby exposing the core which is a single-hinged fold (Fig. 5, section bb'). As a result, the two hinge surface traces of the box fold, when traced southward, converge to form a single trace in the southern half of the body. The fold limbs remain parallel for most of their length within the body. Where they are parallel, the bedding strike in each limb is parallel, the fold is cylindrical, and there is little or no plunge to the fold (maximum plunge does not exceed 2–3 degrees N or S).

The terminations, on the other hand, are non-cylindrical. They resulted from one limb in the body of the fold changing its trend to NW–SE and joining the other limb, which maintained its N–S trend, thus causing the fold to acquire a plunge. In the northern termination, the roof of the box fold diminishes gradually due to the down-plunge convergence of the two hinge lines until they join and the fold becomes single-hinged with a plunge to the NW. In the southern termination, there are two hinge lines that converge southward. The one which represents the continuation of the single-hinged fold of the southern half of the body, trends roughly N–S, plunges mainly to the S, and is cut by a WSW-dipping fore-limb thrust (Fig. 5, section ff'). The other hinge line trends NW–SE, plunges to the NW, and at one locality is cut by a fore-limb minor thrust dipping gently to the E (Fig. 5, sections

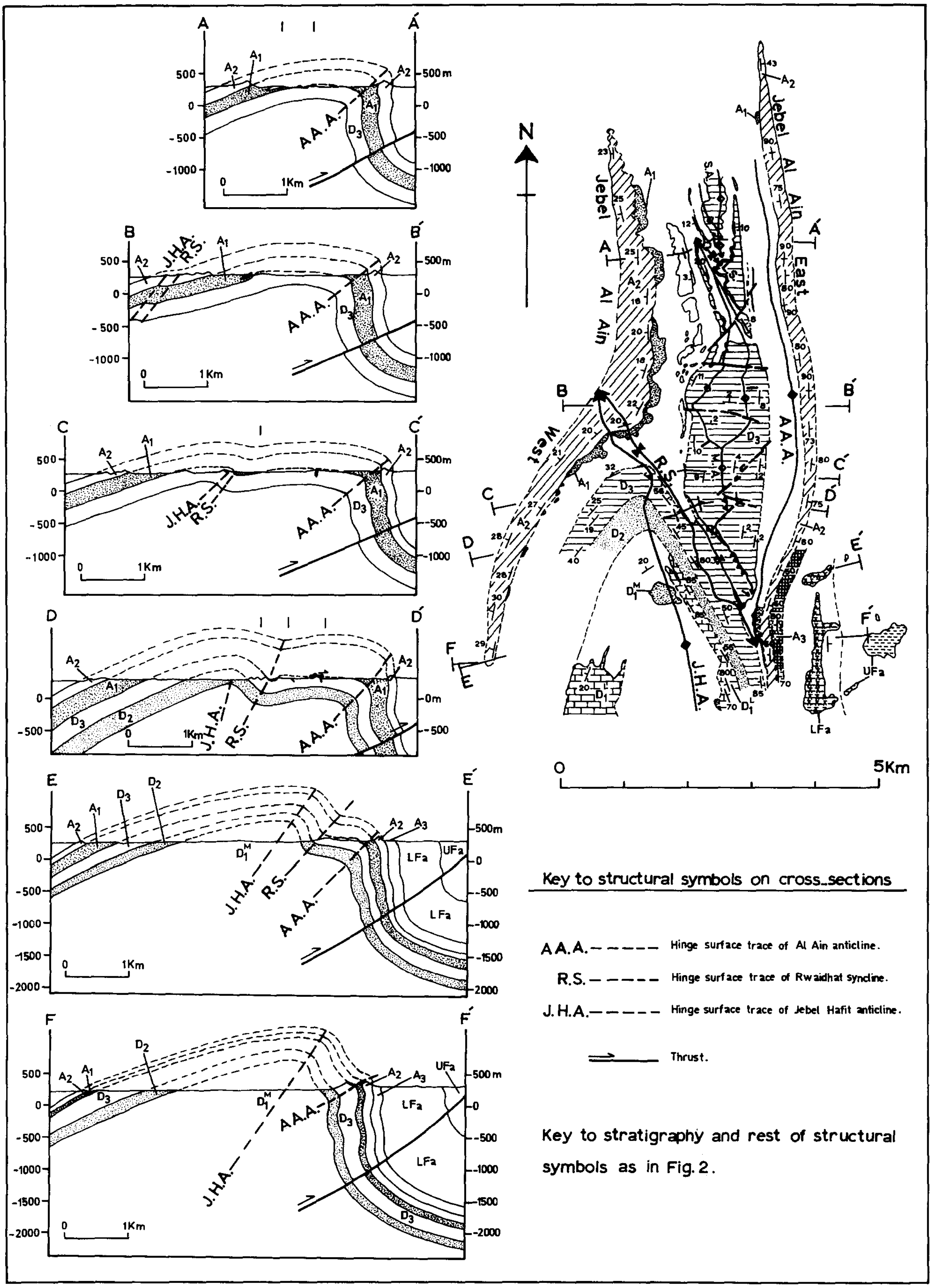

Fig. 4. Geological map and cross-sections of the Al Ain anticline (AA.A.), showing its geometry and relationship to the Jebel Hafit anticline (J.H.A.).

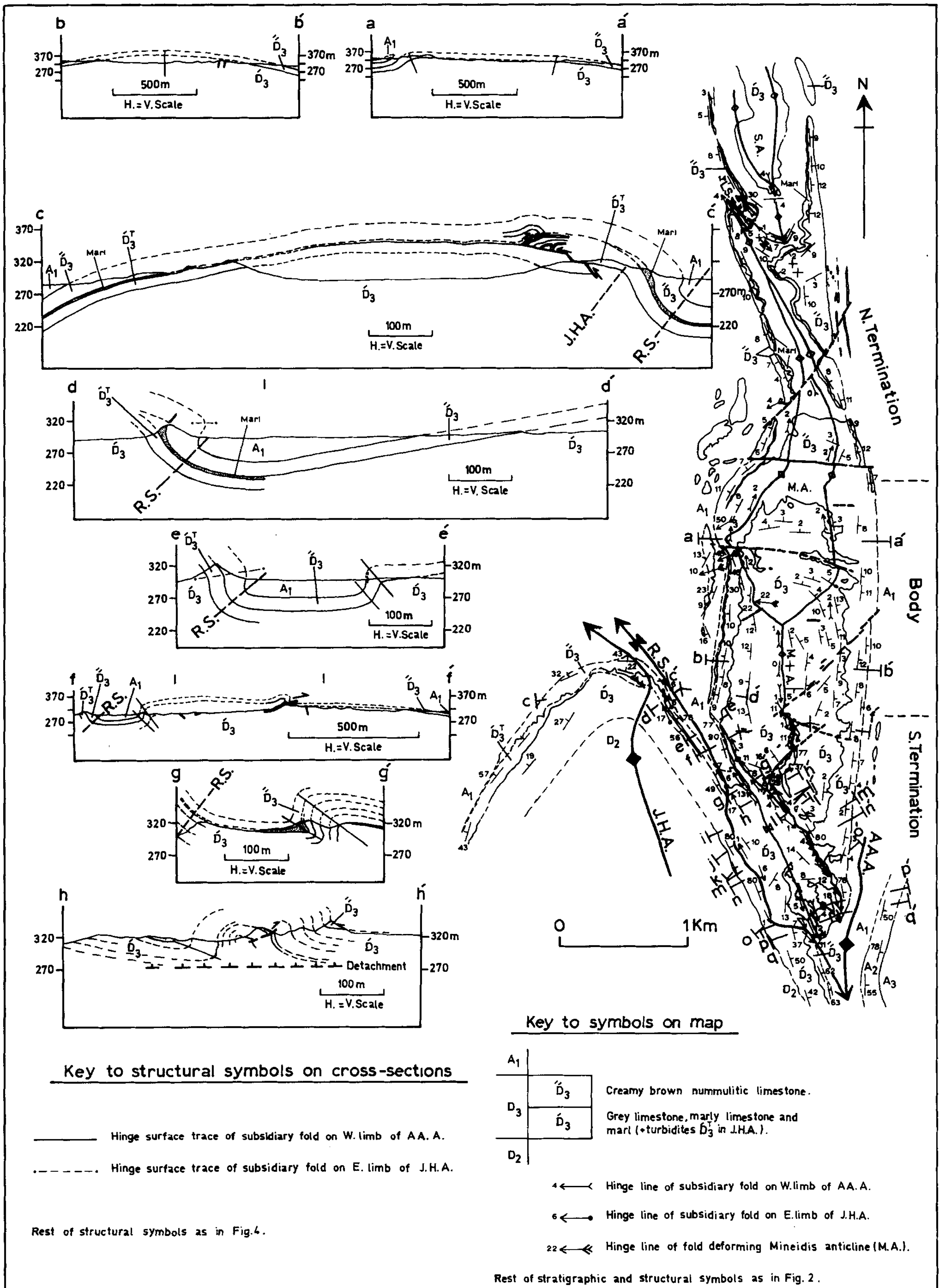

Fig. 5. Geological map and cross-sections of the subsidiary folds superposed on the western limb of the Al Ain anticline.

from ee′ to hh′ and Fig. 6, sections from ii′ to ll′). Once the two hinge lines join, the resulting fold is an asymmetrical, NE-facing anticline that plunges to the SE and is cut by a fore-limb thrust along most of its length (Fig. 6, sections mm′, nn′ and oo′). At the tapering end of the termination, this anticline is replaced by a series of smaller folds that are upright and plunging to the SE (Fig. 6, sections pp′ and qq′). The opposing plunges along the NW–SE trend follow the plunge pattern of the adjacent Rwaidhat linking syncline, and seem to be a reflection of the original attitude of the bedding on which these subsidiary folds were superposed.

The geometry of the Mineidis anticline has been modified by conjugate strike-slip faults that displace the limbs and hinge lines, and by gentle folds which refold the northern half of its western limb (Fig. 5).

Safrah anticline and Leetags syncline

The Safrah subsidiary anticline has a geometry which is similar to that of the Mineidis anticline. It consists of a cylindrical, N–S trending body which is also a box fold with parallel limbs, and a non-cylindrical southern termination plunging sub-horizontally to the S (Fig. 5). The syncline linking the Mineidis and Safrah subsidiary anticlines, the Leetag syncline, is an asymmetric fold that changes its plunge from gentle to the NW to sub-horizontal to the SE after passing through the horizontal at a culmination point. At its NW end, the Leetag syncline has the form of a composite conjugate fold with rounded hinge zones (box form), but toward the SE, it opens out and disappears within a relatively short distance along trend in the brown limestone of the Late Eocene (D''_3; Fig. 5).

Finally, the geometry of the three subsidiary folds as described above, and as shown in the map and cross-sections of Figs. 5 and 6, indicates that this type of folding is shallow, affecting only a thin panel of sediments in the upper part of D_3. It also requires the pres. ıce of two detachment horizons above and below the folded panel. The upper detachment lies within the Asmari lower marl (A_1), which has been removed by erosion, while the lower detachment is located in the incompetent marl just below the tightly folded and thrusted core of the southern termination of the Mineidis subsidiary anticline (Figs. 5 and 6, sections hh′–oo′). The predicted elevation of the lower detachment plane, based on the fold geometry (Dahlstrom 1970), varies from 275 to 300 m above sea-level.

INTERPRETATION

Mechanism of folding

In the Hafit folds, the near constant orthogonal thickness of the folded units as shown in the profile sections, points to a mechanism of buckling largely by tangential longitudinal strain, although flexural slip may have been locally significant as shown by the presence of fibrous slickensides (fibre lineation) on the gypsum veins sandwiched between the bedding in the lower part of D_3. The occurrence of these slickensides oblique to the hinge line may have resulted from the folds being non-cylindrical (Price & Cosgrove 1990), since the slickensides are found on the fold limbs within the northern termination of the Jebel Hafit anticline. Further, from analysing the pattern of its conical terminations, non-uniform shortening by buckling and post-buckle flattening is inferred for the Jebel Hafit anticline and is supported by estimates of finite shortening. This model involving non-uniform shortening, which allows individual folds to terminate where shortening locally falls to zero, is in agreement with the pattern of development of experimental non-cylindrical folds that were initiated non-contemporaneously at a number of localities on a horizontal surface shortened by buckling, and which subsequently grew in amplitude, length and number (Dubey & Cobbold 1977). In the case of the Hafit folds, stratigraphical and sedimentological evidence indicates that the Jebel Hafit anticline was initiated as a structural high on the sea floor just before the Middle Eocene, whilst the Al Ain anticline started to form toward the end of the Eocene (Warrak 1987).

3-D geometry and spatial arrangement

The three-dimensional geometry and spatial arrangement of the Hafit folds are a reflection of the processes of random fold initiation at point irregularities within a multilayer, and the interference and linkage of adjacent growing folds. Price & Cosgrove (1990) pointed out that periclinal folds vary in form both along the hinge line and in profile section, from chevron-like at the point of maximum amplitude in the central part of the fold, to rounded towards their ends. Accordingly, the three-dimensional geometry of an isolated multilayer fold could be regarded as occurring within the limits prescribed by an approximately oblate ellipsoidal space with the fold progressively dying out away from its centre, where the maximum amount of deformation is concentrated. Applying this representation to the folds of the Hafit structure, it is possible to construct a schematic diagram of the three-dimensional geometry (excluding the effect of subsequent deformation) and spatial organisation of the Jebel Hafit and Al Ain anticlines which jointly constitute the Hafit structure (Fig. 7). It is clear from Fig. 7 that these two anticlines are not only off-set horizontally, but their centres are also off-set vertically, with the centre of the Al Ain anticline being much deeper than that of the Jebel Hafit anticline.

Further, the spatial arrangement of the Jebel Hafit and Al Ain anticlines is the result of these adjacent anticlines interacting with each other as they amplified. As shown by Price & Cosgrove (1990), the interaction of two adjacent amplifying periclines could be either by linking or overlapping depending on the distance between the two hinges. If the distance is less than half the wavelength

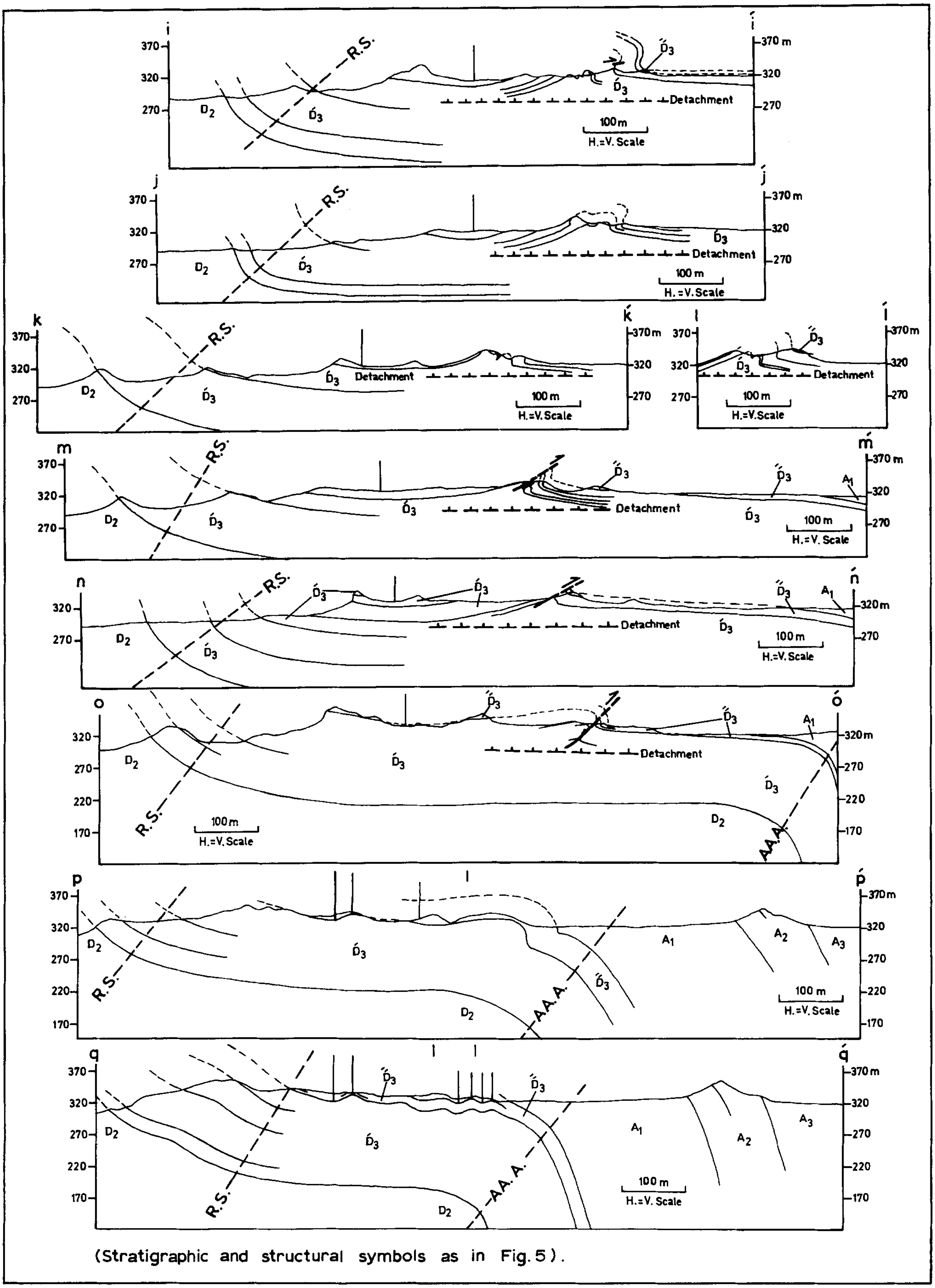

Fig. 6. Serial cross-sections illustrating the geometry of the southern termination of the Mineidis subsidiary anticline. See Fig. 5 for location.

of the fold, oblique linking occurs, but if the distance is greater than half the wavelength, the two anticlines become arranged in an en échelon fashion. In the case of the Hafit structure, the present arrangement of its two anticlines implies that in the folded section below A_2, the two hinges must have been separated by more than half their wavelength so that they became arranged in an en échelon fashion. In the folded section above A_1, however, the distance between their hinges must have become somewhat less than half their wavelength so they linked obliquely to form a larger fold with a deflection in the hinge line. This situation seems to have resulted entirely from their three-dimensional geometry, as a consequence of the increase in wavelength of the two adjoining anticlines at the higher levels of their profile sections (Fig. 7).

Reversed vergence and the subsidiary folds

In the Hafit structure, the reversed vergence and subsidiary folds could have resulted from subsequent modification of the original structure by an ENE-directed rotational strain phase. In the absence of strain markers, this strain could not be specified uniquely: it could be a simple shear or a more general rotational deformation. If plane strain is assumed, however, the geometrical parameters and available field evidence are consistent with a progressive simple shear along shear planes dipping at low angles to the WSW.

It is well known from experimental (Ghosh 1966) and geometrical models (Ramsay *et al.* 1983, Lloyd & Whalley 1986, Ray 1991) that if simple shear strain acts upon an upright symmetrical fold, the fold limbs will undergo changes in shape and orientation depending on their attitude in relation to the incremental strain ellipse for simple shear (Fig. 8a). The fold limb that lies in the shortening field will be shortened and folded, and the limb that lies in the extension field will be stretched and thinned or boudinaged (Fig. 8b). The hinge lines of the buckle folds that form on the shortened limb will generally not be parallel to the hinge line of the pre-existing fold, unless the hinge line of the latter was initially parallel to the shear plane. Thus, during progressive simple shear, the fold limbs rotate further, with the right limb becoming steeper and the left limb gentler. The hinge lines of the folds that formed on the shortened limb and the pre-existing fold will rotate towards the shear plane and both are likely to be periclinal (Lloyd & Whalley 1995, written communication). Normal faulting in the opposite direction to the sense of shear may occur on the fold limbs when they rotate into the field of extension of the incremental strain ellipse. The sheared fold may also exhibit double hinges due to the migration of the hinge point away from the initial hinge surface.

The geometrical models developed by the author using a card-deck simple shear box have shown that, in order to replicate the present geometry of the Jebel Hafit anticline, it is necessary to start with an asymmetrical fold overturned to the west, with a large sub-horizontal fold superposed on its western limb, which formed due to an earlier modification of an upright symmetrical fold by tangential simple shear directed towards the west (Fig. 9a). This fold was subsequently modified by an eastward-directed progressive simple shear strain. During this modification, the two limbs of the fold would rotate at different rates in a clockwise fashion, and the conical terminations would be flattened downwards. The eastern limb would become steep or overturned and shortened, with the development of sub-horizontal buckle folds on it, and the western limb would be stretched and become gently dipping to the west. The former sub-horizontal fold which was superposed on the western limb by the earlier shear movement, would unfold to form the present monoclinal flexure, found at the top of the western limb (Fig. 9b and cross-section BB′ in Fig. 11). Evidence of extension on the western limb includes the

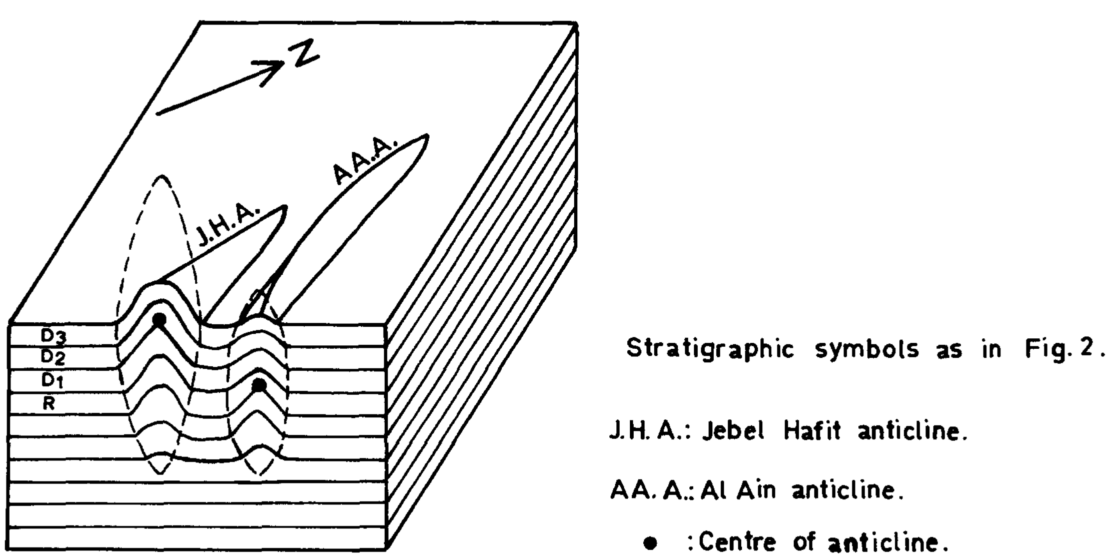

Fig. 7. Schematic representation of the three-dimensional geometry (excluding the effect of subsequent deformation) and spatial arrangement of the Jebel Hafit and Al Ain anticlines.

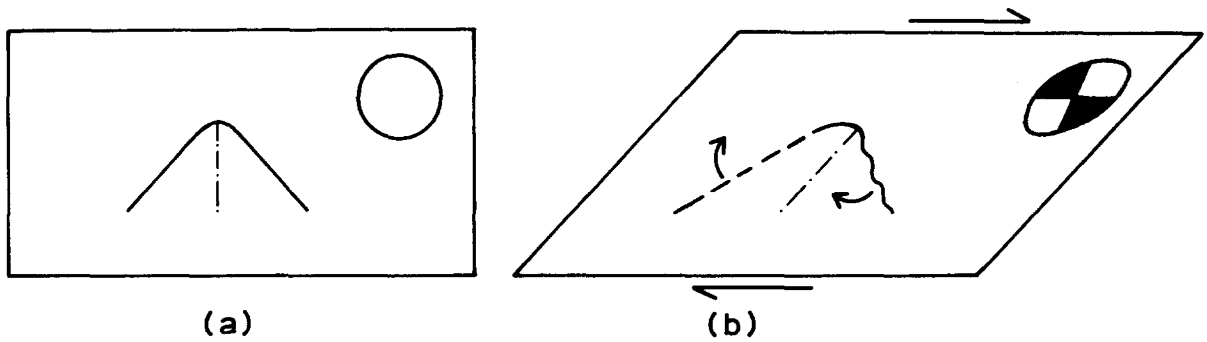

Fig. 8. The effect of dextral simple shear strain on an upright symmetrical fold. (a) The initial attitude of the fold. (b) After an increment of simple shear strain. The fold has become asymmetrical with an inclined hinge surface. The limb which occupies the extension field (shown white on the incremental strain ellipse) is stretched and boudinaged, and the limb that occurs in the shortening field (shown dark on the incremental strain ellipse) is shortened and buckled. Arrows indicate sense of rotation of fold limbs.

widespread development on that limb of structures like pinch-and-swell, boudinage and bedding-parallel stylolites, and the occurrence of steeply WSW-dipping normal faults especially in the crestal zone.

As for the Al Ain anticline, the geometrical models have shown that the initial fold must have been a symmetrical or quasi-symmetrical upright open fold with its western limb oriented at a low angle to the overall simple shear plane, and the eastern limb making a higher angle with it (Fig. 9c). As a result of the simple shear movement, low-amplitude gentle folds (the subsidiary folds) and a gently westward-dipping thrust would initiate on the suitably oriented part of the western limb (crestal zone), whilst the eastern limb would shorten by buckling to form gentle sub-horizontal folds (Fig. 9d and cross-section AA′ in Fig. 11). With the continuation of the shear movement, the eastern limb would rotate and become steeper, but the folds developed on the western limb may suffer downward flattening due to the increased inclination of the axis of compressive strain component of the simple shear.

ORIGIN

The model

The proposed model consists of a multilayer which is lubricated along its base and subjected to one-sided lateral compression. As demonstrated by a photo-elastic experiment (Blay *et al.* 1977), the generated lateral compressive stress propagates forward through the flat-lying multilayer behind a slow-moving stress front. A detachment fold (McClay 1992), may initiate and amplify

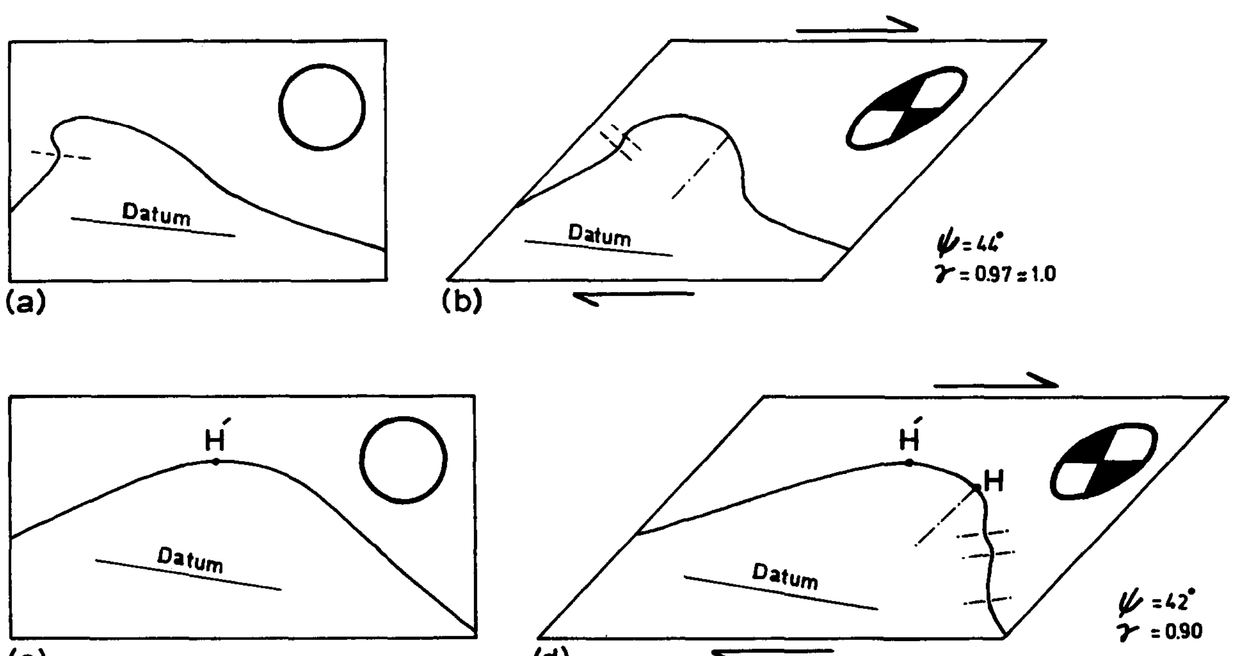

Fig. 9. Possible models showing the suggested initial geometries of the anticlines of the Hafit structure, and their final geometries after modification by dextral simple shear strain. (a) and (b): The Jebel Hafit anticline; (a) suggested initial geometry, (b) final geometry after modification by shear strain $\gamma = 1$. (c) and (d) The Al Ain anticline; (c) suggested initial geometry, (d) final geometry after modification by shear strain $\gamma = 0.9$. Note the double hinges H and H′ of the resulting fold. The fields of extension (white) and shortening (dark) are shown on the incremental strain ellipse for simple shear.

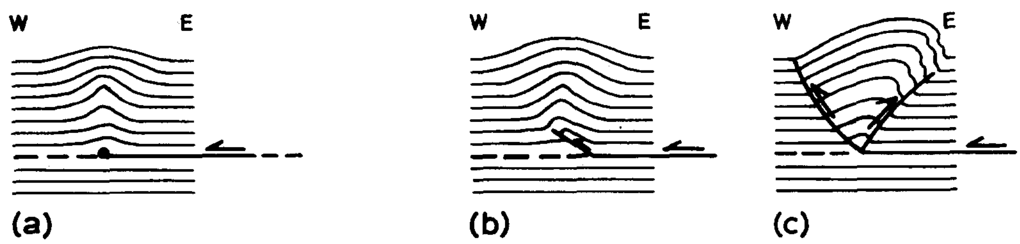

Fig. 10. Simplified illustrations of the model for the origin of the Hafit folds. (a) A detachment fold is initiated and amplified above a point on a decollement surface where the stress front is temporarily arrested during its stick-slip mechanism of propagation. (b) The stress built up behind the arrested wave-front is relieved through the development of a listric thrust from the basal decollement to accommodate further shortening. (c) Modification of the fold geometry and formation of an antithetic back thrust as a result of the rotation of the hangingwall as it moves up the frontal footwall ramp.

above a point on the decollement surface where the stress front is temporarily arrested during its stick-slip mechanism of forward propagation (Fig. 10a). The stress built up behind the arrested wave-front may be relieved through the development of a listric thrust, which propagates upwards from the basal decollement plane to accommodate further shortening (Fig. 10b). As a result of the rotation of the hangingwall as it moves up this listric thrust, a rotational strain is induced in the hangingwall with the development of an antithetic back thrust, which becomes steeper with depth (Mandl & Crans 1981). This rotational strain would modify the geometry of the detachment fold causing it to face eastward and to have subsidiary folds superposed on its limbs (Fig. 10c).

Mode of origin

The Jebel Hafit anticline may have been initiated as an upright symmetrical pericline just before the Middle Eocene, due to one-sided compression from the ENE. After reaching a certain amplitude, it was probably modified to an asymmetrical fold overturned to the west by a westward-directed tangential simple shear strain, which was generated within the folded panel due to differential displacement between its upper and lower parts (cf. Ramsay & Huber 1987). Towards the end of the Eocene, a symmetrical or quasi-symmetrical open periclinal fold (Al Ain anticline) started to grow to the NE of the Jebel Hafit pericline. As both periclines amplified and grew in length, they at first overlapped in an en échelon fashion, and later (after the Early Oligocene) linked obliquely to form a larger anticlinal structure with a curved hinge line.

To relieve a temporary arrest in the ability to propagate westward, the basal decollement which is probably located in the Upper Cretaceous Lower Fiqa shale, branches into a listric east-dipping thrust that cuts up section to accommodate further shortening. As the hangingwall climbs up this listric thrust, an eastward-directed progressive simple shear is induced in it with the development of an antithetic back thrust (confirmed by drilling, Hunting 1979) that becomes steeper with depth. This shear movement which must have continued until the end of the Miocene, is considered responsible for the reversed vergence of the folds and the superposition of subsidiary folds on their limbs as described before (Fig. 11).

TIMING OF DEFORMATION

In the Northern Oman Mountains, two main compressional events have been recognised. The first event resulted from the obduction of the Semail ophiolite onto the Arabian margin during the Coniacian to Lower Maastrichtian. This obduction created a widespread compressional deformation and the flexural foredeep of the Late Cretaceous Aruma Basin (Glennie *et al.* 1974, Searle *et al.* 1983, Searle 1988b, Nolan *et al.* 1990, Dunne *et al.* 1990). The second compressional event was post-obduction and caused major folding and short-distance thrusting of the whole autochthonous and allochthonous package as well as the neoautochthonous (Upper Cretaceous and Teriary) sediments (Ricateau & Riché 1980, Searle *et al.* 1983, Searle 1985, Dunne *et al.* 1990). The large-scale periclinal folds fringing the western edge of the Northern Oman Mountains (including the Hafit and related structures in the Al Ain region) and the westward thrusting of the Musandam shelf carbonates sequence over the allochthonous Hawasina cherts, have all resulted from this event, which has been dated Mid–Late Tertiary (late Eocene–Miocene) and correlated with the deformation of the Zagros fold belt of SW Iran (Ricateau & Riché 1980, Searle *et al.* 1983, Searle 1985). However, in spite of the agreement amongst geologists about the general timing and the sequence of the main compressional events, there are still ambiguities in the exact timing and number of structural reactivation events of the post-obduction deformation (Dunne *et al.* 1990).

The stratigraphical and sedimentological evidence from the Al Ain region (Warrak 1987) has shown that the Hafit and related structures to the east of it developed serially in time from east to west, and that their deformation was contemporaneous with sedimentation. The folds to the east of the Hafit structure started to grow at the beginning of the Palaeocene, whilst the Hafit structure was initiated just before the Middle Eocene and continued to grow synchronously with sedimentation until the end of the Miocene. Further, the base Tertiary unconformity identified in the subsurface of the Hafit

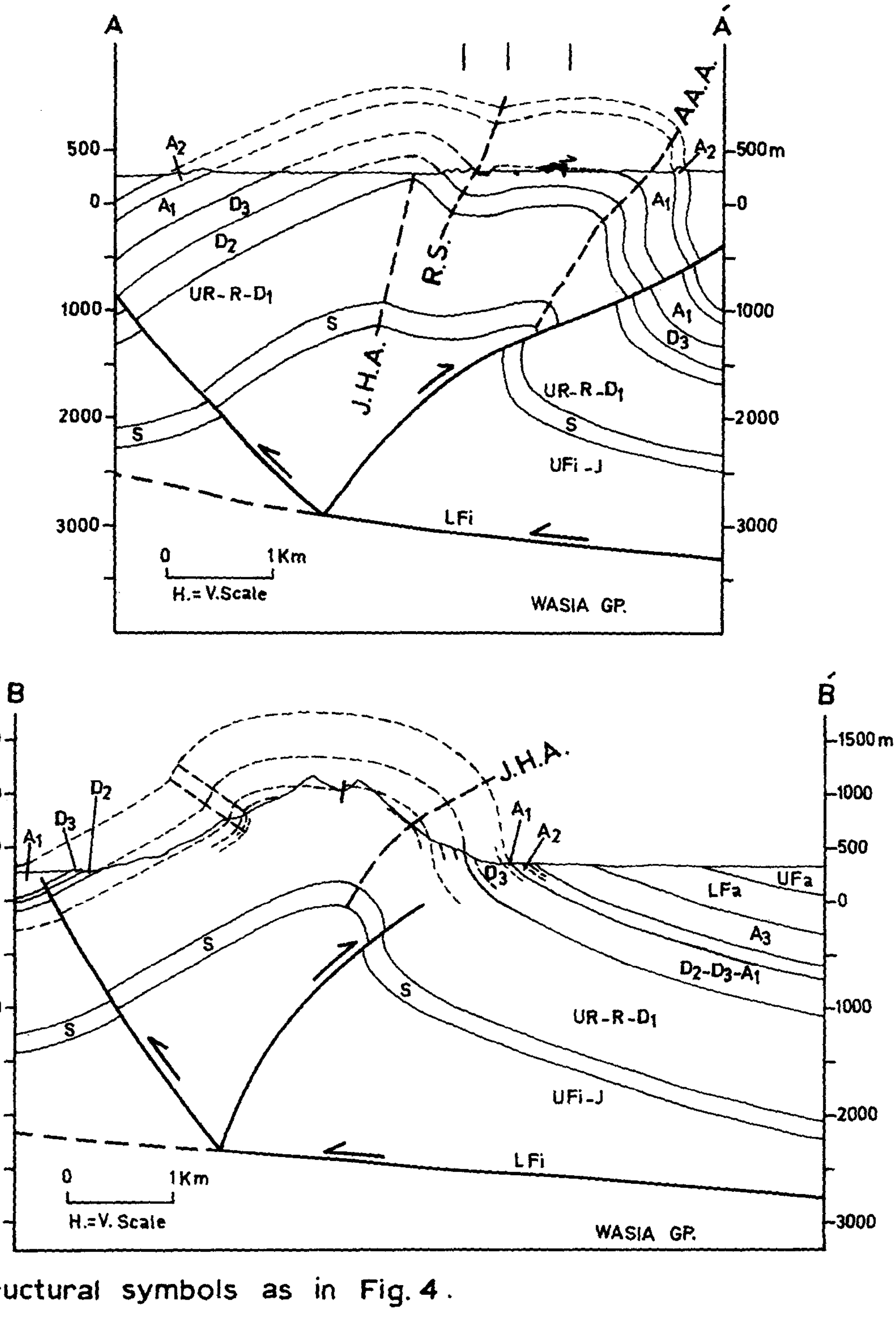

Structural symbols as in Fig. 4.

Symbols of stratigraphic units as in Table 1 and Fig.2.

Fig. 11. Interpretative cross-sections of the Hafit structure. The presence of back thrust is known from drilling (Hunting 1979), whilst the lower parts of the sections are based on theoretical and geometrical characteristics of the proposed model. See Fig. 2 for location.

area and which correlates with a similar event to the north (Nolan *et al.* 1990), has been interpreted by Boote *et al.* (1990) to indicate early Tertiary tectonism. Farther to the north, detailed mapping and structural analysis by the author of Upper Cretaceous and early Tertiary rocks at the western end of the Hatta zone (Jebel Rawdha), have revealed that strong movements occurred on the Hatta shear zone during the Palaeocene–Middle Eocene, which controlled the sedimentation and facies of these rocks. Also, Searle (1988b) in his study of the Musandam peninsula concluded that the thrust culmination of the Musandam must have occurred after the late Cretaceous, probably coinciding with flexural downwarping of the Palaeocene–Eocene Pabdeh foreland basin, and prior to the Upper Miocene which unconformably overlies Tertiary thrust tip lines offshore in the Gulf (Ricateau & Riché 1980).

This evidence makes it necessary to push back the time of initiation of the second compressional event in the Northern Oman Mountains to the beginning of the Palaeocene, and to define the time span of this deformation to be from the beginning of the Palaeocene to the end of the Miocene, thus setting it apart from the Zagros deformation, which began in very late Miocene and culminated in the Late Plio-Pleistocene (Stocklin 1968, Murris 1980). Deformation of the Oman margin had largely ceased by this time, apart from mild uplift, accompanied by underthrusting of the Musandam promontory along the Zendan fault zone (White & Ross 1979, Ross *et al.* 1986). It should be pointed out here that the distinction between this second compressional event which produced the Hafit structure, and the Zagros deformation, is based only on the difference in timing, and does not reflect differences in the structural style of their folds. In fact, there are many geometrical and structural similarities between the foreland folds of the Northern Oman Mountains and the Zagros folds, e.g. both are large-scale periclinal structures that are underlain by decollement surfaces.

Finally, the proposal by Boote *et al.* (1990) that the folds along the Oman margin (including the Hafit structure) resulted from southward-directed transpressional deformation along deep basement fractures due to the indentation of the Musandam promontory into the Iranian crustal collage in post-early Miocene, although plausible, does not account for the early Tertiary tectonism observed in the Hafit and other parts of the Northern Oman Mountains.

CONCLUSIONS

(1) The Hafit structure was formed as a result of one-sided compression acting from the ENE. This compression produced an array of en échelon periclines that developed serially in time from east to west in the flat-lying folded panel. The Hafit structure, being one of these folds, grew as a detachment fold above a decollement surface which is probably located in the Upper Cretaceous Lower Fiqa shale.

(2) The reversed (ENE) vergence, back thrust and the folds superposed on the limbs of the Hafit folds, are all explained as being due to simple shear modification of the original structure as it moved up a listric, east-dipping thrust plane that branched up from the basal decollement.

(3) The interpretation that the Hafit structure and other foreland folds in the Northern Oman Mountains have resulted from a Zagros-related late Eocene–Miocene compressional event, is at variance with the stratigraphical and sedimentological evidence from the Hafit area. This evidence shows that the Hafit structure grew synchronously with sedimentation from just before the Middle Eocene until the end of the Miocene, whilst the related structures to the east of it were initiated at the beginning of the Palaeocene.

(4) With more evidence of a similar early start to the Tertiary deformation emerging from the Hafit area and other parts of the Northern Oman Mountains, it becomes necessary to push back the initiation of the Tertiary compressional event to the Palaeocene and to set it apart from the Plio-Pleistocene Zagros deformation.

Acknowledgements—I wish to thank J. G. Ramsay and K. W. Glennie for reviewing the manuscript and providing helpful comments and suggestions. I also wish to thank the referees M. P. Searle and G. E. Lloyd for their criticism of this paper, and in particular Geoff Lloyd for sending me the latest Lloyd and Whalley's manuscript on simple shear modification of chevron folds. Special thanks to my colleagues A. R. A. Hamdan, H. S. Anan and S. A. Bahr for their numerous discussions on the stratigraphy of the Hafit structure. Help with the research facilities provided by the U.A.E. University is also acknowledged.

REFERENCES

Blay, P., Cosgrove, J. W. & Summers, J. M. 1977. An experimental investigation of the development of structures in multilayers under the influence of gravity. *J. geol. Soc. Lond.*, **133**, 329–342.

Boote, D. R. D., Mou, D. & Waite, R. I. 1990. Structural evolution of the Suneinah Foreland, Central Oman Mountains. In: *The Geology and Tectonics of the Oman Region* (edited by Robertson, A. H. F., Searle, M. P. & Ries, A. C.). *Spec. Publs geol. Soc. Lond.* **49**, 397–418.

Cherif, O. H. & El Deeb, W. M. Z. 1984. The Middle Eocene–Oligocene of the Northern Hafit area, south of Al Ain City (United Arab Emirates). *Géol. Médit.*, **11**, 207–217.

Coleman, R. G. 1981. Tectonic setting for Ophiolite Obduction in Oman. *J. geophys. Res.*, **86**, 2497–2508.

Dahlstrom, C. D. A. 1970. Structural geology in the eastern margin of the Canadian Rocky Mountains. *Bull. Can. Petrol. Geol.* **18**, 332–406.

Dubey, A. K. & Cobbold, P. R. 1977. Noncylindrical flexural slip folds in nature and experiment. *Tectonophysics*, **38**, 223–239.

Dunne, L. A., Manoogian, P. R. & Pierini, D. F. 1990. Structural style and domains of the Northern Oman Mountains (Oman and United Arab Emirates). In: *The Geology and Tectonics of the Oman Region* (edited by Robertson, A. H. F., Searle, M. P. & Ries A. C.). *Spec. Publs geol. Soc. Lond.* **49**, 375–386.

Ghosh, S. K. 1966. Experimental tests of buckling folds in relation to strain ellipsoid in simple shear deformation. *Tectonophysics*, **3**, 169–185.

Glennie, K. W., Boeuf, M. G. A., Hughes Clarke, M. W., Moody-Stuart, M., Pilaar, W. F. H. & Reinhardt, B. M. 1974. Geology of the Oman Mountains. *Verh. K. Ned. geol. Mijnb. Genoot.*, **31**, 1–423.

Hamdan, A. R. A. & Bahr, S. A. 1992. Lithostratigraphy of the Paleogene succession of northern Jabal Hafit, Al Ain area, United Arab Emirates. *M.E.R.C. Ain Shams Univ. Earth Sci. Ser.*, **6**, 201–224.

Hunting (Geology and Geophysics Ltd) 1979. Report on a Mineral Survey of the U.A.E., Al Ain Area. *Ministry of Petroleum and Mineral Resources, Abu Dhabi* **9**, 1–29.

Lloyd, G. E. & Whalley, J. S. 1986. The modification of chevron folds by simple shear: examples from north Cornwall and Devon. *J. geol. Soc. Lond.*, **143**, 89–94.

Mandl, G. & Crans, W. 1981 Gravitational gliding in deltas. In: *Thrust and Nappe Tectonics* (edited by McClay, K. R. & Price N. J.). *Spec. Publs geol. Soc. Lond.* **9**, 41–54.

McClay, K. R. 1992. Glossary of thrust tectonics terms. In: *Thrust Tectonics* (edited by McClay, K. R.). Chapman and Hall, London, 419–433.

Murris, R. J. 1980. Middle East: Stratigraphic evolution and oil habitat. *Bull. Am. Assoc. Petrol. Geol.*, **64**, 597–618.

Nicol, A. 1993. Conical folds produced by dome and basin fold interference and their application to determining strain: examples from North Canterbury, New Zealand. *J. Struct. Geol.* **15**, 785–792.

Nolan, S. C., Skelton, P. W., Clissold, B. P. & Smewing, J. D. 1990. Maastrichtian to early Tertiary stratigraphy and palaeogeography of the Central and Northern Oman Mountains. In: *The Geology* *and Tectonics of the Oman Region* (edited by Robertson, A. H. F., Searle, M. P. & Ries A. C.). *Spec. Publs geol. Soc. Lond.* **49**, 495–519.

Patton, T. L. & O'Connor, S. J. 1988. Cretaceous flexural history of Northern Oman Mountain Foredeep, United Arab Emirates. *Bull. Am. Assoc. Petrol. Geol.*, **72**, 797–809.

Price, N. J. & Cosgrove, J. W. 1990. *Analysis of Geological Structures.* Cambridge University Press, Cambridge, U.K.

Ramsay, J. G., Casey, M. & Kligfield, R. 1983. Role of shear in development of the Helvetic fold-thrust belt of Switzerland. *Geology*, **11**, 439–442.

Ramsay, J. G. & Huber, M. I. 1987. *The Techniques of Modern Structural Geology. V.2: Folds and Fractures.* Academic Press, London.

Ray, S. K. 1991. Significance of forelimb folds in the Shumar allochthon, Lesser Himalaya, Eastern Bhutan. *J. Struct. Geol.*, **13**, 411–418.

Ricateau, R. & Riché, P. H. 1980. Geology of the Musandam peninsula (Sultanate of Oman) and its surroundings. *J. Petrol. Geol.*, **3**, 139–152.

Ross, D. A., Uchupi, E. & White, R. S. 1986. The geology of the Persian Gulf — Gulf of Oman region: a synthesis. *Rev. Geophys.*, **24**, 537–556.

Searle, M. P. 1985. Sequence of thrusting and origin of culminations in the northern and central Oman Mountains. *J. Struct. Geol.*, **7**, 129–143.

Searle, M. P. 1988a. Thrust tectonics of the Dibba zone and the structural evolution of the Arabian continental margin along the Musandam mountains (Oman and United Arab Emirates). *J. geol. Soc. Lond.*, **145**, 43–53.

Searle, M. P. 1988b. Structure of the Musandam culmination (Sultanate of Oman and United Arab Emirates) and the Straits of Hormuz syntaxis. *J. geol. Soc. Lond.*, **145**, 831–845.

Searle, M. P., James, N. P., Calon, T. J. & Smewing, J. D. 1983. Sedimentological and structural evolution of the Arabian continental margin in the Musandam Mountains and Dibba zone, United Arab Emirates. *Bull. geol. Soc. Am.* **94**, 1381–1400.

Stocklin, J. 1968. Structural history and tectonics of Iran: a review. *Bull. Am. Assoc. Petrol. Geol.* **52**, 1229–1258.

Warburton, J., Burnhill, T. J., Graham, R. H. & Isaac, K. P. 1990. The evolution of the Oman Mountains Foreland Basin. In: *The Geology and Tectonics of the Oman Region* (edited by Robertson, A. H. F., Searle, M. P. & Ries A. C.). *Spec. Publs geol. Soc. Lond.* **49**, 419–27.

Warrak, M. 1986. Structural evolution of the Northern Oman Mountains front, Al Ain region. In: *Hydrocarbon Potential of Intense Thrust Zones* (Proceedings of Abu Dhabi Symposium). *Ministry of Petroleum and Mineral Resources, U.A.E. and Organisation of Arab Petroleum Exporting Countries, Kuwait* **1**, 375–31.

Warrak, M. 1987. Synchronous deformation of the neoautochthonous sediments of the Northern Oman Mountains. In: *Proceedings of SPE 5th Conference, Bahrain*, 129–136.

Webb, B. C. & Lawrence, D. J. D. 1986. Conical fold terminations in the Bannisdale Slates of the English Lake District. *J. Struct. Geol.*, **8**, 79–86.

White, R. S. & Ross, D. A. 1979. Tectonics of the western Gulf of Oman. *J. geophys. Res.*, **84**, 3479–3489.